Polymer 50 (2009) 2743–2751

Contents lists available at ScienceDirect

Polymer

journal homepage: www.elsevier.com/locate/polymer

Polymer mediated formation of corona-embedded gold nanoparticles in block polyelectrolyte micelles

Anastasia Meristoudi [a,b], Stergios Pispas [a,*]

[a] Theoretical and Physical Chemistry Institute, National Hellenic Research Foundation, 48 Vassileos Constantinou Avenue, Athens 116 35, Greece
[b] University of Patras, Department of Materials Science, Patras 26 504, Greece

ARTICLE INFO

Article history:
Received 24 February 2009
Received in revised form
10 April 2009
Accepted 19 April 2009
Available online 3 May 2009

Keywords:
Block copolymer micelles
Metal nanoparticles
Nanoparticle formation kinetics

ABSTRACT

Micelles having a hydrophobic core of poly(*tert*-butylstyrene) and a hydrophilic corona of poly(sodium sulfamate/carboxylate-isoprene) anionic polyelectrolyte, were formed through self-assembly of the diblock copolymer poly[*tert*-butylstyrene-*b*-sodium (sulfamate/carboxylate-isoprene)] (BS-SCI) in water. $HAuCl_4$, as the metal precursor, was preferentially dissolved and coordinated into the corona of the micelles. Au nanoparticles were formed within the corona block by subsequent reduction of Au^{3+} to Au^0 without introducing any reducing agent, since the amine group of the corona block acts as both the reducing and stabilizing agent. The kinetics of the Au reduction reaction was followed by UV–vis spectroscopy by direct observation of the exact position and the intensity of the surface plasmon resonance band of created Au nanoparticles. The colloidal stability and structural response of the BS-SCI/Au nanohybrid was studied as a function of pH, ionic strength and temperature by dynamic light scattering (DLS). Additional information on the structure of the hybrid systems and the metal nanoparticle characteristics were gathered by UV–vis spectroscopy, atomic force microscopy (AFM) and transmission electron microscopy (TEM). Taking into account the polyelectrolyte nature and biocompatibility of the SCI corona of the BS-SCI/Au nanoassembly, the interactions with a model globular protein (lysozyme) were investigated, aiming at exploring the potential application of such hybrid colloids in protein assay protocols.

1. Introduction

Gold nanoparticles (AuNPs) have attracted significant attention due to the catalytic, electric, optical and photonic properties that they exhibit, depending on their size, shape and the surrounding medium [1–3]. This holds also for other metal nanoparticles but AuNPs are frequently utilized as a model case [1]. The synthesis of gold nanoparticles, usually involves their incorporation into matrices such as surfactants, copolymers or dendrimers [4,5], which act as stabilizers in order to avoid agglomeration due to van der Waals forces [6–8]. However, the reports on the preparation of gold nanoparticles usually involve the addition of a reducing agent which may create undesired byproducts [9,10,11]. An important challenge remains the development of simple and environmental friendly methods for the synthesis of gold nanoparticles of controlled size and shape [12]. Such methods, could allow for the gold nanoparticles to be widely used in biological systems, for instance as an alternative for fluorophores in biolabeling [13] and in bio(macro)molecular determination/detection assays or even in cancer diagnostics and therapy [14] due to their interesting optical properties.

Recently, polymers that have amino or hydroxyl groups are used in order to overcome the disadvantages mentioned above. Amines are used as reducing and stabilizing agents in AuNP formation, although it is not clear which amine properties, chemical or structural, are responsible for their reducing character [15]. However, it is known that the reduction of $HAuCl_4$ to Au^0 occurs due to the electrons transferred from the amine to the metal ion. Then, the metallic Au undergoes nucleation and growth in order to form Au nanoparticles [15]. On the other hand, main chain ether polymers, with hydroxyl terminal functionalities, can form pseudocrown ether cavities in the presence of cations [16], encapsulating thus metal cations and subsequently promoting their reduction to metallic nanoparticles.

Iwamoto et al. used water soluble diamine terminated polyethylene oxide (PEO-NH_2), which was mixed with $HAuCl_4$ and heated at 100 °C, in order to produce gold nanoparticles of good colloidal stability, with an average diameter of 16 nm [11].

Aslam et al. reported the formation of an Au–amine complex for the production of Au nanoparticles. The Au–amine complex was so rapidly thermally decomposed that the AuNPs formed

* Corresponding author. Tel.: +30 210 7273824; fax: +30 210 7273794.
E-mail address: pispas@eie.gr (S. Pispas).

0032-3861/$ – see front matter © 2009 Elsevier Ltd. All rights reserved.
doi:10.1016/j.polymer.2009.04.045

were protected by the amine groups preventing any aggregation [17]. More recently, branched poly(ethyleneimine) (PEI) was used, as both the reducing and the stabilizing agent, for the formation of Au nanoparticles at room temperature [18]. By varying the amount of PEI initially used, the size of the AuNPs formed could be controlled.

AuNP formation in the presence of block copolymer micelles is another widely used strategy in order to produce colloidally stable nanoparticles of controllable size and introduce chemical functionality in the final hybrid nanocolloids [19]. Alexandridis et al. in one of their studies, showed that poly(ethylene oxide)-*b*-poly (propylene oxide) (PEO-*b*-PPO) block copolymer could act as the reducing, stabilizing and morphogenic agent at the one pot synthesis of Ag and Au nanoparticles [20]. In another work [21], the same group reported the size and shape controlled synthesis of colloidal gold through autoreduction of $AuCl_4^-$ by PEO-*b*-PPO block copolymers in aqueous solutions at ambient temperature. However, the studies so far mainly concern the formation of AuNPs into micellar cores of amphiphilic block copolymers of already nanostructured systems [8,22], where the cores are regarded as nanoreactors for the nucleation and growth of AuNPs. Thus, some of the properties that gold nanoparticles display (i.e. catalytic) may be inhibited or compromised because they are embedded in the dense micellar core.

An effective strategy in order to overcome such deficiencies would be to fix the Au nanoparticles either on the corona or the shell of the micelle. This is particularly important when the catalytic properties of the metal nanoparticle are targeted, since in this case access of the substrate to the nanoparticle active surface is greatly enhanced. Fixing the AuNPs at the corona of the micelle could also allow for interaction with biological molecules. If the biological molecules have a functional group which can bind to the AuNP surface, a ligand exchange reaction can occur, replacing the stabilizer molecules by the biological ones [23] and the optical properties of the AuNPs may be modulated.

Shi et al. proposed the formation of Au–micelle composite within a core-shell-corona structure in organic solvents [24]. They first prepared micelles consisting of a poly(ethylene oxide) core and a Au/poly(4-vinylpyridine) corona. Addition of polystyrene-*b*-poly(4-vinylpyridine) led to the formation of a multifunctional hybrid material comprised of a PEO core, a swollen Au/P4VP shell, which is very sensitive to pH conditions [25], and a PS corona. However, a reducing agent was necessary for the formation of the AuNPs into the P4VP shell.

In another study, gold nanoparticles were covalently conjugated onto the periphery of thiol functionalized thermosensitive poly (*N*-isopropylacrylamide) (PNIPAM) unimollecular micelles in order to fabricate satellite-like nanostructures. These micellar templates were able to shrink and swell reversibly in response to thermal treatment. Consequently, the spatial distances between gold nanoparticles attached at the micelles surface, could be altered [26]. Block copolymer micelles with metal nanoparticle decorated corona have been prepared by micellar structure inversion due to a change in the solvent from micelles containing the nanoparticles initially in their cores [27,28]. Another closely related field of research is the metal nanoparticle synthesis or their immobilization into spherical or planar polymer brushes [29–31]. Spherical polyelectrolyte brushes can be used for the immobilization of proteins in order to obtain functional systems [32]. Strong adsorption of bovine serum albumin (BSA) onto the spherical polymer brushes has been observed despite the fact that both BSA and the particles were negatively charged [33].

Combining the ability of spherical polyelectrolyte brushes to interact with proteins and the optical properties and biocompatilbily of AuNPs, could allow for the formation of more complex nanostructures which could be used in sensor applications [34,35], i.e. by monitoring the plasmon resonance frequency of AuNPs [36,23], since it is highly influenced by the binding of molecules onto the particle surface [37].

In an attempt to amplify and further explore the trend in Au/block copolymer nanohybrid synthesis we utilized poly[*tert*-butylstyrene-*b*-sodium (sulfamate/carboxylate-isoprene)] (BS-SCI) diblock copolymer micelles for the synthesis of Au nanoparticles in water. H_2O is a selective solvent for the anionic SCI block, leading to the formation of well-defined micelles consisting of a hydrophobic core (BS) and a hydrophilic corona (SCI). Furthermore, varying amounts of $HAuCl_4$ were added, as the metal precursor, which were preferentially dissolved and coordinated to the corona of each micelle and subsequently reduced, by the amino groups of the corona block, to Au nanoparticles. The dispersion stability and responsivity of the BS-SCI/AuNPs hybrid nanostructures were evaluated in detail under various conditions, i.e. temperature, pH, ionic strength by means of dynamic light scattering (DLS) and UV–vis absorption spectroscopy. Additional structural information on the hybrid systems and the metal nanoparticles was gathered by atomic force microscopy (AFM) and transmission electron microscopy (TEM). Finally the interaction between the BS-SCI/Au nanoensemble and lysozyme were investigated in order to explore the possibility of utilization of such nanomaterials in protein assays.

2. Experimental section

2.1. Materials

$HAuCl_4$ was synthesized by dissolving Au 99.99% in HCl/HNO_3 (3:1) and then diluting the red residue into ethanol, in order to yield a 0.03 M solution. Lysozyme from hen egg white ($M_r = 14{,}600$ and pI = 11.0), purchased from Fluka, was used as received.

The poly[(*tert*-butylstyrene-*b*-isoprene)] (BS-I) precursor diblock copolymer was synthesized by anionic polymerization high vacuum techniques [38,39], by sequential addition of *tert*-butylstyrene and isoprene in a solution of sec-BuLi in benzene, ensuring narrow molecular weight distribution of the final block copolymer. It was subsequently transformed to poly[*tert*-butylstyrene-*b*-sodium (sulfamate-carboxylate-isoprene)] (BS-SCI) block polyelectrolyte by reaction with chlorosulfonylisocyanate, which transforms the polyisoprene block of BS-I to an anionic polyelectrolyte, as was reported previously [40]. The precursor and final block copolymers were thoroughly characterized in terms of molecular weights, composition and chemical functionality by a combination of size exclusion chromatography, ^1H and ^{13}C NMR, ATR–FTIR, potentiometric titration and elemental analysis. Molecular characterization results confirmed the desired structure of the BS-SCI block polyelectrolyte (i.e. $M_{w,\,BS\text{-}SCI} = 1.64 \times 10^5$, $M_{w,\,BS\ block} = 1.97 \times 10^4$, $M_w/M_n = 1.03$, 12 wt% poly(*tert*-butylstyrene) content, 75% functionalization of the polyisoprene block). The structure of the block polyelectrolyte utilized in this study is shown in Scheme 1.

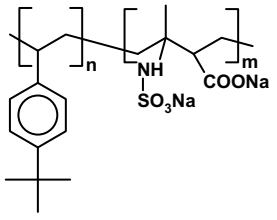

Scheme 1. Chemical structure of the BS-SCI block polyelectrolyte utilized in this study.

2.2. Micelle formation

Micelle formation has taken place in distilled water where the BS-SCI block copolymer was dissolved in order to prepare polymer solutions with concentration of 10 mg/mL. Solutions of lower copolymer concentration were prepared by dilution of the stock solutions (typical concentration range studied 1–10 mg/mL). Since poly(*tert*-butylstyrene) is extremely hydrophobic, dissolving BS-SCI in H_2O is expected to lead to formation of micelles with a BS core and a SCI corona. The preparation of solutions took place at room temperature.

2.3. Preparation of the hybrid metal–polymer solutions

To prepare hybrid micellar solutions, the obtained micellar solutions were mixed with 0.5 and 0.25 equiv. of $HAuCl_4$ per amine unit, which was dissolved and preferentially coordinated at the micellar corona. The colour of the solutions was progressively changing in a period of 18 h from uncoloured transparent to red/dark red depending on the concentration of the polymer and $HAuCl_4$. After 18 h and at room temperature, the metal salt was completely reduced by the corona block and the colour of the solutions changed to dark red, and thereafter no changes were observed. The dispersions displayed good colloidal stability over a period of months. A schematic illustrating the preparation protocol is given in Scheme 2.

2.4. Kinetics of Au^{3+}reduction and stability studies

The kinetics of the reduction of Au^{3+} to Au^0 by the anime group of SCI was studied by mixing $HAuCl_4$ with the hybrid micellar solution at certain molar N/Au ratios, and observing the developing absorption bands by UV–vis spectroscopy, under heating the resulting solution at 50 °C or at room temperature. UV–vis spectra from the mixed solutions were collected every 30 min and for at least 24 h after the addition of $HAuCl_4$, until no considerable changes were observed in the spectra and the reaction was assumed to be completed. The onset of the reaction could be also observed by naked eye through the development of a light pink colour in the solution after 30 min under heating or after 10 h at room temperature.

To investigate the effect of pH on the stability of already formed BS-SCI/Au nanohybrids, the initial pH of the aqueous hybrid solution was adjusted from 6.3 to 3.3 by adding 0.1 M HCl solution and to pH = 10.1 by addition of 0.1 M NaOH. The effect of the ionic strength on the system characteristics was evaluated by addition of various quantities of NaCl giving salinities in the range of 0.03–0.2 M.

2.5. Investigation of BS-SCI/Au-lysozyme interactions

In order to prepare BS-SCI/Au-lysozyme mixed solutions, a constant volume of BS-SCI/Au solution ($c = 2 \times 10^{-3}$ g/mL, N/Au = 4:1) was mixed with different volumes of an aqueous solution of lyzosyme ($c = 2 \times 10^{-3}$ g/mL). The total volume of the final solutions was adjusted to 10 mL by adding distilled water where necessary. The concentration of the BS-SCI/Au nanohybrid was fixed to 1×10^{-4} g/mL through the series of the solutions (ionic strength 0.01 M and pH = 6.3), while the lysozyme concentration of the final solutions was in a range of 1×10^{-5} g/mL to 1×10^{-3} g/mL. The mixed solutions were allowed to stand for 24 h at room temperature for equilibration before measurements. In Scheme 3 the complex formation between the BS-SCI/Au hybrid nanocolloid and lysozyme is depicted.

All samples were transparent with a light pink colour due to the presence of Au nanoparticles, except for the samples containing 2×10^{-4} g/mL and 1×10^{-3} g/mL lysozyme respectively, which were blurry and impossible to filter through the 0.45 μm filter.

2.6. Characterization methods

Dynamic light scattering (DLS) was employed in order to follow the behaviour of the Au/block polyelectrolyte nanosystems as well as their interactions with lysozyme. Measurements were performed on a ALV/CGS-3 Compact Goniometer System (ALV GmbH, Germany), equipped with a JDS Uniphase 22 mW He–Ne laser, operating at 632.8 nm, interfaced with a ALV-5000/EPP multi-tau digital correlator with 288 channels and a ALV/LSE-5003 light scattering electronics unit for stepper motor drive and limit switch control. The scattering intensity and correlation functions were measured in the angular range of 45°–135°. Correlation functions were collected for fives times in each angle and were analyzed by the cumulant method and the CONTIN software, which provides the apparent hydrodynamic radii distributions by Laplace inversion of the correlation function and by aid of the Stokes–Einstein relationship. All solutions were filtered through a 0.45 μm Millipore

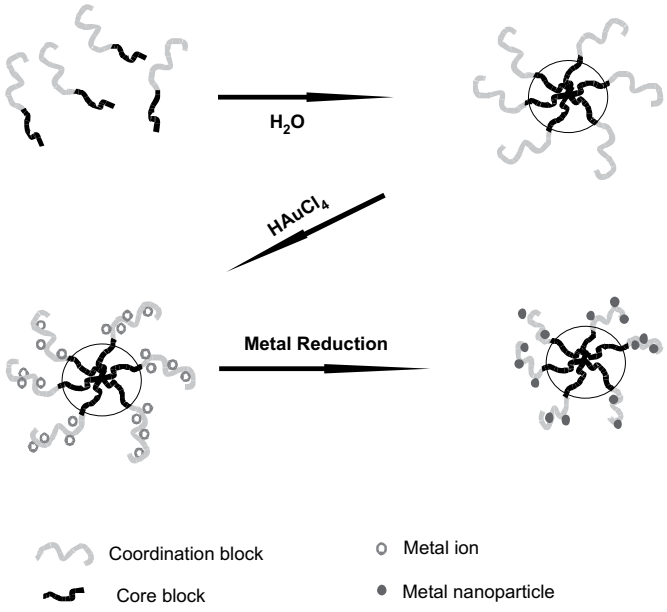

Scheme 2. Schematic showing the preparation protocol for metal nanoparticle/block copolymer hybrid assemblies based on the BS-SCI block copolymer in water.

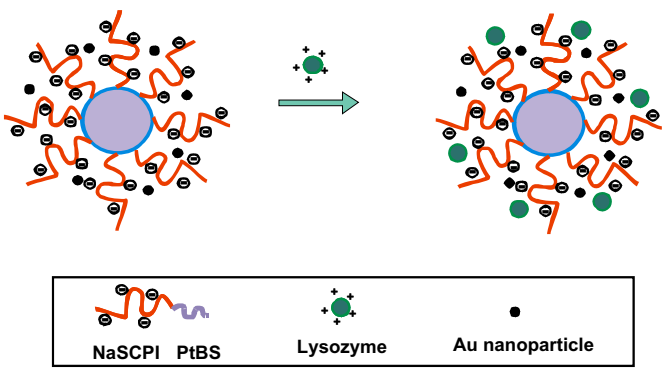

Scheme 3. Schematic showing the preparation protocol for metal nanoparticle/block copolymer/protein hybrid.

LCR hydrophilic Teflon filter into dust free cylindrical light scattering cells (diameter 1 cm) [8].

Solutions were also characterized by UV–vis spectroscopy using a Perkin–Elmer UV–vis/NIR Lamda 19 spectrometer. The UV–vis spectra were collected in the range of 350–1100 nm with a data interval of 1 nm and a scan speed of 489 nm/min. Transmission electron microscopic (TEM) images were taken on a JEOL model JEM100C electron microscope, operated at 80 kV accelerating voltage and under bright field conditions. Samples for TEM imaging were prepared by depositing a drop of the solutions onto carbon-coated EM copper grids. Approximately five minutes after the deposition, the excess of solution was blotted away with a strip of filter paper and the rest was allowed to dry at room temperature.

Atomic force microscopic (AFM) images were obtained in the tapping mode with a scanning probe microscope (VEECO SPM Multimode). The samples were prepared by a similar method as those for the TEM, however, the deposition of the hybrid nanocolloid solutions was done onto fresh, methanol precleaned silicon wafers.

3. Results and discussion

3.1. SCI mediated synthesis of Au nanoparticles in the corona of BS-SCI micelles

As already mentioned the BS block displays high hydrophobicity, while SCI block is hydrophilic. Dissolving BS-SCI in water leads to the formation of micelles with BS cores and SCI coronas. DLS was used in order to follow the self-assembling behaviour both of the micelles and the Au loaded hybrid micelles. In Fig. 1, the distribution of hydrodynamic radii is shown, after analysis of the intensity correlation function by CONTIN and conversion to intensity weighted hydrodynamic radii distributions [8]. Only one distinct diffusing species is present, with a hydrodynamic radius of 111 nm, which is attributed to the formation of block copolymer micelles.

After the addition of $HAuCl_4$ and the subsequent reduction of Au^{3+} to metallic gold, within 24 h, the hydrodynamic radius decreased remarkably. The coordination of the Au nanoparticles within the micelle's corona leads to a more compact conformation of the hybrid material. Once the metal precursor is added in the micelles solution, complexation of $AuCl_4^-$ with the SCI blocks in the corona of the micelles occurs, causing the corona chains to contract. Then, the reduction of Au^{3+} to Au^0 is facilitated by the amine groups of the SCI block [11] and according to the DLS measurements, the polymer chains become more compact, leading to complex micelles with a hydrodynamic radius of 90 nm and 67 nm for addition of 0.25 equiv. and 0.5 equiv. of Au^{3+} per amine group respectively. Addition of a larger amount of gold ions causes a larger contraction of the corona chains resulting in an overall smaller size of the micelles. This finding also suggests that the increase of Au loading forced the corona chains to adjust their conformation, probably causing some agglomeration of the AuNPs and surely shortening the distances between the gold cores [41,42] within the corona. However, a second species was observed upon addition of 0.5 equiv. of Au per amine units, displaying an R_h of 16 nm. This may be attributed to small gold fragments which did not coordinate with the SCI block in the block copolymer micelles and were formed within the unimer chains that are present in the solution. The presence of unimers is now evident due to the enhancement of contrast due to Au coordination.

The formation of gold nanoparticles through reduction driven by the amine groups of the BS-SCI block copolymer in aqueous solutions was followed by observing the intensity of the absorption bands centered at ~527 nm and originating from the surface plasmon resonance of the gold nanoparticles developing in the system. Fig. 2 shows the absorption spectra obtained after mixing the aqueous solution of the BS-SCI block copolymer with $HAuCl_4$ and heating at 50 °C (N/Au = 4:1). The spectra were collected every 30 min and an increase in the intensity of the absorption band was observed with no observable significant changes in the position of the maximum. This indicated that the gold nanoparticles were formed by the amine reduction of $AuCl_4^-$, which was enhanced due to the thermal treatment. Under these conditions the process was completed after about 2.5 h. Only minor increases in absorption occurred thereafter.

In the absence of thermal treatment, the reduction reaction was slower and gold nanoparticles were slowly formed, with an absorption peak appearing at 10 h after mixing the BS-SCI block copolymer and $HAuCl_4$ solutions and taking up to 24 h until the reduction was completed (as deduced by the SPR band attaining a plateau level). This indicates that raising the temperature, even at a moderate level, can considerably accelerate the chemical reduction process. Absorption maxima are centered at the same wavelength independent of the use of heating or not. This indicates that AuNPs of the approximately the same size are formed in each case. Once the reduction process is completed and the formation of gold

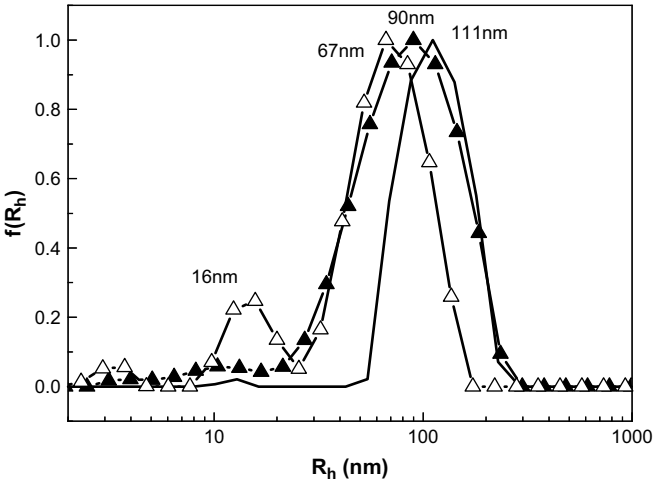

Fig. 1. Hydrodynamic radius distribution for BS-SCI micelles in water (solid line), BS-SCI/Au^0, N:Au = 4:1 (closed triangles) and BS-SCI /Au^0 N:Au = 2:1 (open triangles).

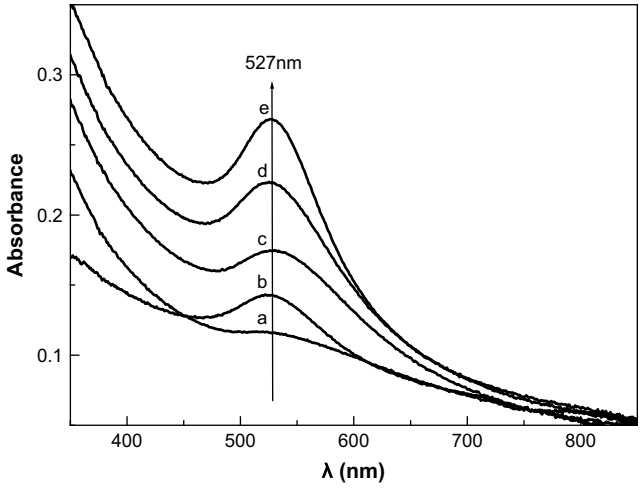

Fig. 2. Absorption spectra of BS-SCI/Au^0 N:Au = 4:1 colloid. The arrow follows the increase in the absorption maximum, centered at ~527 nm, due to the SPR of gold nanoparticles formed after heating the colloid solution at 50 °C for (a) 30 min, (b) 60 min, (c) 90 min, (d) 120 nm, (e) 180 min.

nanoparticles is accomplished, the hybrid BS-SCI/Au micelles show no thermal response and the AuNPs remain stable without forming any aggregates (or precipitants) even after heating for 3 h at 50 °C. However, increasing the quantity of $HAuCl_4$ added, from 0.25 to 0.5 equiv. versus amine groups, led to a red shift of the absorption band [21,25] (Fig. 3). The SPR shift could be attributed to the formation of nanoparticle cluster of greater size, because of nanoparticle agglomeration, due to a larger quantity of gold utilized.

Since gold nanoparticles are not trapped inside highly viscous micellar cores, but they exist coordinated to the corona block, they interact with one another and they can form aggregates. Also, this shift could be due to the lower N:Au ratio used, as it is believed that when the concentration of the reducing agent used is low, larger particles are formed [18]. The experimental results show that it is possible to control the size of the nanoparticles formed by changing the N:Au ratio within the micellar corona.

In order to obtain further information on the structure of the hybrid BS-SCI/Au complex, AFM measurements were performed. A representative image is shown in Fig. 4, for the case of N:Au 4:1. The nanostructures seem well-defined on the SiO_2 surface with a nearly spherical shape. The size of the hybrid BS-SCI/Au complex obtained from AFM is smaller than that obtained by DLS (an average diameter of ~80 nm was derived from AFM versus that of ~180 nm derived from DLS).

However, it should be taken into account that AFM measurements were made in absence of any solvent, which in fact plays a major role in the swelling of the micellar corona and thus affecting the measured size of the micelles in solution by DLS. Any aggregates observed could be attributed to interactions of the complex material with the surface [43] during and after the solvent evaporation.

A TEM image of the BS-SCI/Au micelles is shown in Fig. 5, where the micelles show a uniform spherical morphology with an average diameter of 53 nm. Once again the size of the micelles measured by DLS is much larger than that derived by TEM, since the microscopy result is obtained for the micelles in the dry state in which the polymer chains have collapsed, while in DLS measurements the polymer chains remain swollen or stretched due to the presence of solvent. Large aggregation of primary micelles was evident on the TEM grid because of solvent evaporation and micelle/substrate interactions. Furthermore, the differences in the sizes measured by TEM and AFM should be attributed to the different measurement modes of the two techniques and primarily to the effective contrast present in the TEM case.

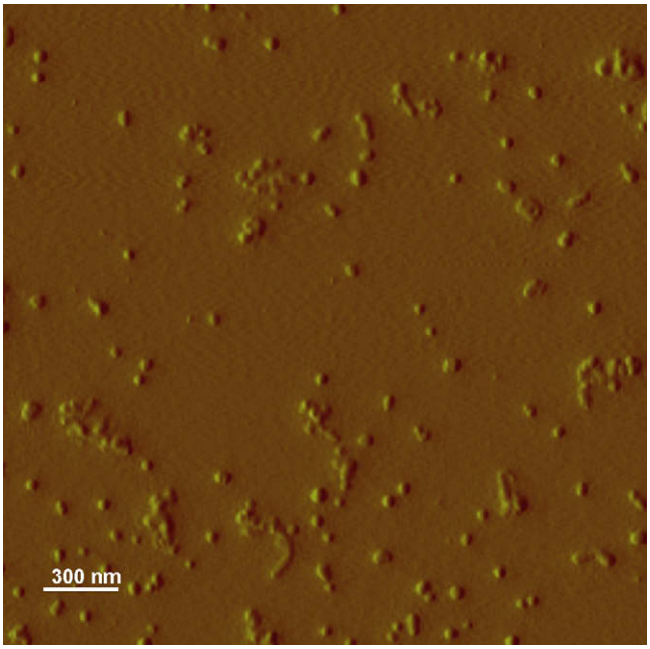

Fig. 4. AFM image of the BS-SCI/Au^0 N:Au = 4:1 hybrid micelles.

In a close up view (inset in Fig. 5) small gold nanoparticles surrounding the BS-SCI micelle can be observed. The gold nanoparticles are rather monodisperse, with a uniform spherical size. Sizes, shape and distribution of the AuNPs from TEM are in agreement with the UV–vis spectra obtained, which suggested the formation of spherical AuNPs with diameter less than 15 nm [1]. The images in the insets of Fig. 5 are consistent with the formation of AuNPs in the micellar corona of BS-SCI aqueous micelles.

3.2. Effect of ionic strength and pH on the properties of BS-SCI/Au hybrid micelles

Since the corona of BS-SCI micelles is comprised of a polyelectrolyte block the effect of salt on the structural characteristics and optical properties of the hybrid micelles was also investigated, both by DLS and UV–vis spectroscopy. This information is important since biological applications of the hybrid micelles can be

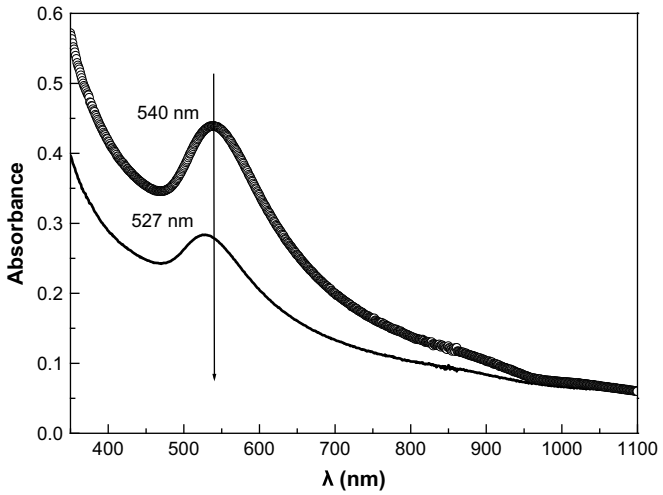

Fig. 3. Absorption spectra of BS-SCI/Au^0 N:Au = 4:1 (solid line) and BS-SCI/Au^0 N:Au = 2:1 (circles) hybrid solutions.

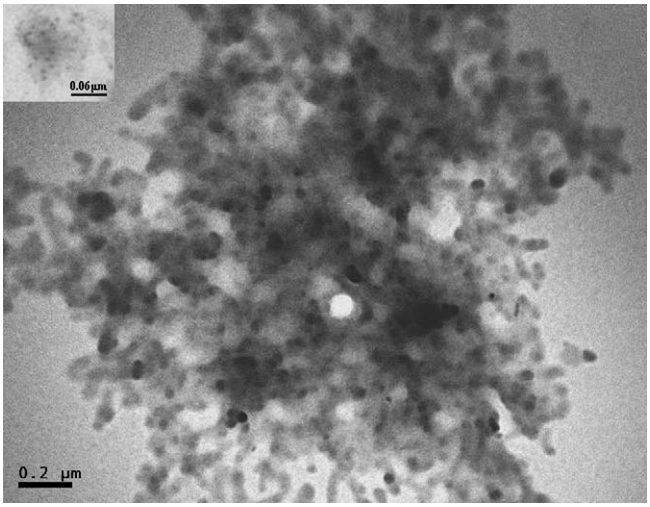

Fig. 5. TEM images of the BS-SCI/Au^0 N:Au = 4:1 hybrid micelles. Inset is a higher magnification of an isolated hybrid micelle.

envisioned. A colloid dispersion of the BS-SCI/Au (N:Au 4:1) hybrid was prepared and various quantities of NaCl were added, so as to gradually increase the salt concentration from 0.03 M to 0.2 M. Altogether, three salt concentrations were studied (0.03 M, 0.1 M and 0.2 M) in order to investigate the effect of ionic strength on the hybrid colloidal system. When 0.03 M NaCl was added to the solution, a prompt increase in the absorbance band was observed (Fig. 6), probably due to the contraction of the corona in the presence of salt, which in turn affects the distances between metal nanoparticles and apparently changes their environment. Gradual addition of NaCl (up to 0.1 M and 0.2 M) led to a subsequent decrease of the absorption band centered at ~527 nm due to gold nanoparticles' plasmon resonance. This decrease can be also tentatively attributed to changes in the environment surrounding the AuNPs. A more detailed explanation of this complex behaviour is impossible at the moment. Nevertheless, the phenomenon may be useful in applications.

However, upon addition of 0.2 M NaCl (the highest concentration of salt studied) a shoulder at around ~827 nm was observed. The second absorption peak at longer wavelengths is consistent with the presence of anisotropic agglomerates of nanoparticles within the micellar corona [1], as the ionic strength of the system increases. Probably, as the salt concentration in the solution increases, a second order aggregation of the AuNPs occurs, due to the contraction of the polyelectrolyte corona blocks, as a result of screening of electrostatic interactions [44].

In Fig. 7 the apparent hydrodynamic radii of the same BS-SCI/Au hybrid micelles upon addition of varying quantities of NaCl are depicted. As examined by DLS, the addition of NaCl to the system, leads to a decrease in the size of the micelles. Before salt addition the R_h was 90 nm (for the N:Au 4:1 molar ratio) but as NaCl was added R_h was decreased to 74 nm (Fig. 7), implying a shrinkage of the block copolymer micelle. This is to be expected due to the polyelectrolyte nature of the corona SCI block [44]. In the presence of salt electrostatic interactions within the corona are screened and result in the contraction of the corona chains.

It should also be noted that the intensity increased and it was almost doubled for the case of 0.2 M NaCl. The change in the scattering intensity is rather small in order to be attributed to a secondary aggregation of the micelles (in any case such an event would lead to an increase in the measured dimensions of the system). Therefore, it must be due to the enhancement of the scattering contrast, owing to the agglomeration of the AuNPs as a result of the contraction of the corona SCI blocks. Thus the addition of salt in the BS-SCI/Au colloids leads to a change in size of the hybrid particles and to changes in the optical properties of the suspension. The behaviour of the polyelectrolyte BS-SCI upon addition of NaCl, in the absence of AuNPs, was investigated by DLS, as a control experiment. An overall decrease in the size of the BS-SCI micelles was monitored, due to the presence of NaCl, as expected for polyelectrolyte brushes [44]. However, the contraction is higher compared to the case of BS-SCI/Au micelles (an R_h equal to 67 nm was determined for pure BS-SCI micelles in aqueous solutions with NaCl concentrations in the range 0.03–0.5 M). Apparently, the presence of gold nanoparticles inhibits the maximum collapse of the corona chains in BS-SCI/Au micelles.

In order to investigate the pH effects on the properties of the BS-SCI/Au hybrid micelles, the initial pH value of the aqueous solution was adjusted by addition of HCl or NaOH as described in the Experimental section. In Fig. 8 the hydrodynamic radius distributions are depicted at different values of pH i.e. acidic environment at pH ~3.3 after addition of 0.1 M HCl at the almost neutral initial BS-SCI/Au colloid (pH ~6.3) and alkaline conditions at pH ~10.1

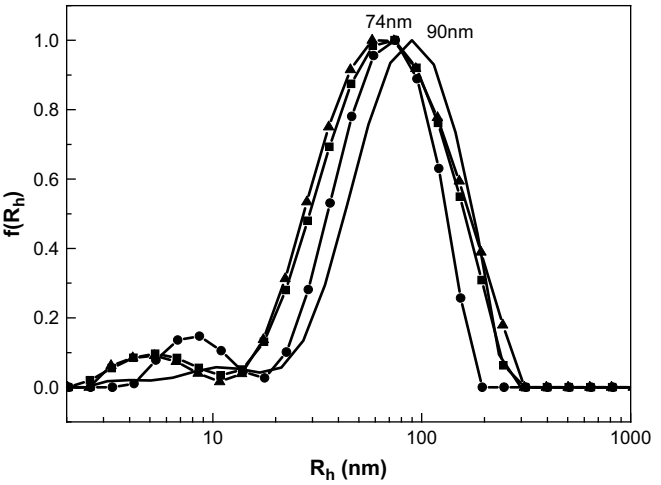

Fig. 7. Hydrodynamic radius distribution for BS-SCI/Au^0 (N:Au = 4:1) (solid line), BS-SCI/Au^0 (N:Au = 4:1)/NaCl 0.03 M (triangles), CSI-BSI/Au^0 (N:Au = 4:1)/NaCl 0.09 M (squares) and CSI-BSI/Au^0 (N :Au = 4:1)/NaCl 0.2 M (circles).

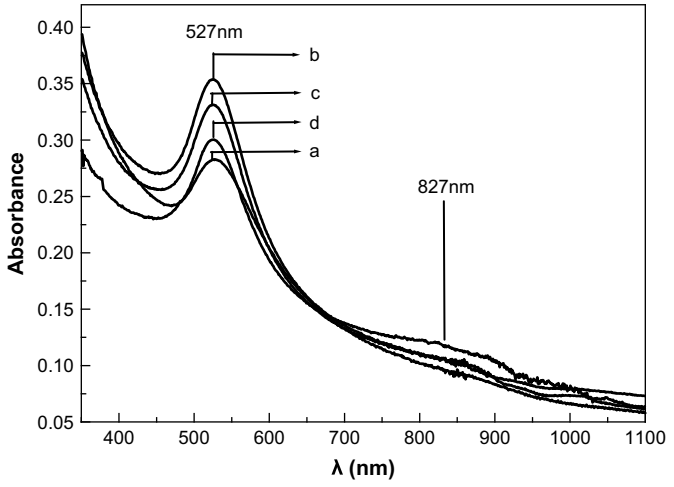

Fig. 6. Absorption spectra of the BS-SCI/Au^0 N:Au = 4:1 hybrid micelles upon addition of NaCl. (a) BS-SCI/Au^0 before any NaCl addition, (b) after addition of 0.03 M NaCl, (c) 0.1 M NaCl and (d) 0.2 M NaCl (see text for details).

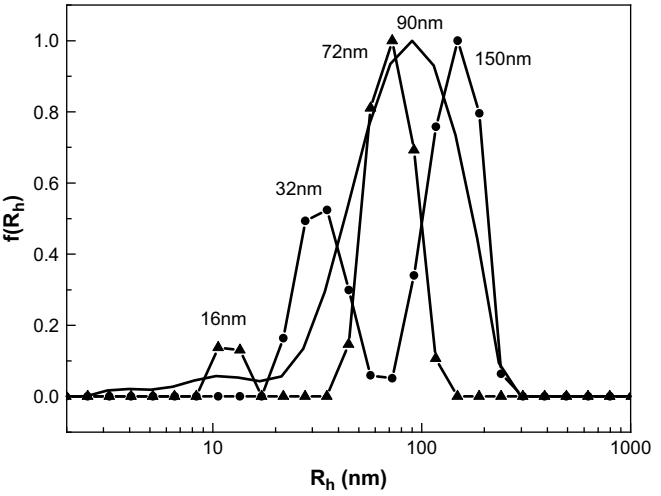

Fig. 8. Hydrodynamic radius distribution for BS-SCI/Au^0 (N:Au = 4:1) at pH 6.3 (solid line), 3.3 (triangles) and 10.1 (circles).

upon addition of 0.1 M NaOH, in comparison to the initial state. It should be noted, that since all pH changes take place after the formation of the AuNPs in the corona of the BS-SCI micelles, no size or shape changes of the AuNPs are expected. Also, any changes observed should be attributed to the changes of the pH of the aqueous solution of BS-SCI/Au, since the pH is the only experimental parameter modified with respect to the initial state. However, it was observed that the changes in pH affected the size distribution of BS-SCI/Au hybrid micelles, as explained below.

The BS-SCI/Au colloid under acidic conditions (pH 3.3) shows a decrease in its size (R_h becomes 72 nm at room temperature) and a more narrow size distribution compared to pH 6.3. The decrease in the R_h could be attributed to the protonation of the carboxylate groups in the SCI block of the copolymer, which leads to a shrinkage of the corona and of the whole micelle, due to the decrease in the charges present on the polyelectrolyte chains. This contraction may also cause the existing AuNPs to come closer together [45]. A second distribution with a hydrodynamic radius of 16 nm was also observed, which could be attributed to unimers as discussed before. Actually, the position of the UV–vis absorption band was red shifted at 535 nm (Fig. 9), indicating also that the distance between the neighbouring AuNPs is decreased [42] due to the shrinkage of the micellar corona. The absence of a second absorption peak at longer wavelengths [1] suggests that changes in the relative positions of the AuNPs within the micellar corona are taking place and not agglomeration of the nanoparticles (in contrast to the case which salt was added to the system).

On the other hand, when the pH was increased to 10.1, a dramatic increase in the R_h was observed (becoming 150 nm) (Fig. 8). Probably this is due to the complete deprotonation of the amino groups of the SCI block of the copolymer, which resulted in an increase of the effective charges on the SCI blocks and a swelling of the corona and the micelles [45] as a whole. A second species was also observed in this case. The R_h of this species was 32 nm, while the contribution of this peak to the total scattering intensity from the solution becomes more prominent compared to the one observed for the same system under acidic conditions (Fig. 8). This peak may be correlated with unimer chains that also increase their size due to pH changes. Additionally, the changes in the protonation state of the groups on the SCI blocks of the BS-SCI/Au hybrid, at pH 10.1, could cause the partial decomposition of some of the micelles (i.e. change in the micelles–unimer equilibrium in favour of the unimers, due to the increased solubility of the block polyelectrolyte), thus justifying the presence of a second more prominent peak in the R_h distribution function. Regarding the UV–vis absorption spectra, a small blue shift (of ~5 nm) of the SPR peak was observed, supporting the suggestion that as the SCI segment gets deprotonated, the micelles swell and the relative distances between the AuNPs increase [42].

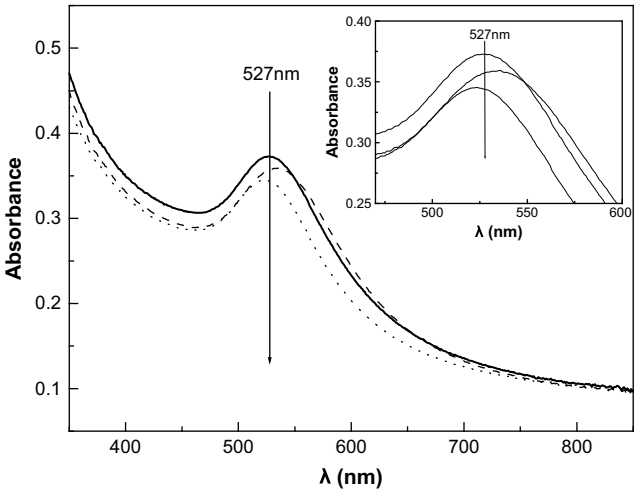

Fig. 9. Absorption spectra for BS-SCI/Au^0 (N:Au = 4:1) at pH 6.3 (solid line), 3.3 (dashed line), and 10.1(dotted line). Inset is a magnification of the region 400–650 nm.

The pH value of the solution was found to be a key factor in the reversible volume phase transition of the BS-SCI/Au hybrid, in contrast to the ionic strength effect. The shift of the exact position of the surface plasmon band, due to the swelling or shrinkage of the corona in the complex hybrid [29], makes the BS-SCI/Au hybrid a potential candidate for the formation of next generation AuNPs [46]. The construction of next generation AuNPs incorporated into or coordinated with smart polymer matrixes, which change their conformation and characteristics in response to pH or the temperature, is believed to be the key factor for the fabrication of bio-tools and bio-devices [46].

3.3. Interaction of BS-SCI/Au hybrid micelles with lysozyme

In an attempt to explore the potential for bioapplications of the present hybrid colloids the self-assembling behaviour and properties of the BS-SCI/Au colloid complexed with lysozyme, a model globular protein, was investigated. The positively charged lysozyme at ca. neutral pH (as is the case for the BS-SCI/Au solutions-measured pH = 6.3) is expected to interact with the negatively charged BS-SCI/Au hybrid micelles, leading to the formation of a more complex material, which consists of a dense hydrophobic BS core and a pH sensitive, hydrophilic SCI shell, which carries Au nanoparticles and is complexed with protein globules (Scheme 3). Solutions of various concentrations in lysozyme were prepared and were studied by means of DLS and UV–vis spectroscopy. In Fig. 10a the average hydrodynamic radius of the BS-SCI/Au/lysozyme colloid is presented as a function of the concentration of lysozyme in the system. The apparent R_h of the BS-SCI/Au hybrid before addition of any lysozyme was 123 nm, while, once a small quantity of lysozyme ($c_{lysozyme} = 1 \times 10^{-5}$ g/mL) was added in the colloidal solution, a decrease of the R_h was observed ($R_h = 113$ nm). Increasing the concentration of lysozyme resulted in a gradual increase of the overall size of the complex colloid particles and almost reached the initial value at a lysozyme concentration of 1×10^{-4} g/mL. The samples which had larger lysozyme concentrations could not be filtered. This experimental observation indicates the presence of micelle agglomeration in the solutions of larger lysozyme concentration (possibly protein mediated interactions lead to secondary aggregation of primary micelles and indeed in some of the solutions precipitation was observed after standing for several days). The trend that the complex BS-SCI/Au/lysozyme displays, regarding the R_h, can be attributed to structural changes that occur in the BS-SCI/Au corona upon lysozyme complexation (an initial shrinking of the corona and a latter increase in its dimensions as more lysozyme is complexed). More specifically, at low lysozyme concentrations, due to the excess of negative charges, complete coordination of the protein around the copolymer/Au hybrid micelle takes place. Due to the complexation, conformational rearrangement of the components of the complex occurs, which lead to a more compact shape with a relatively smaller size. As the lysozyme concentration increases, the hydrodynamic radius of the complexes increases, probably because of a stretched conformation that the SCI chains adopt, in order to allow the positively charged protein molecules to interact with the remaining negative charges and be accommodated within the corona. Moreover, the presence of Au nanoparticles, already coordinated to the SCI chains, prevents lysozyme molecules to approach closely to the corona chains, thus forcing them to adopt a more stretched conformation.

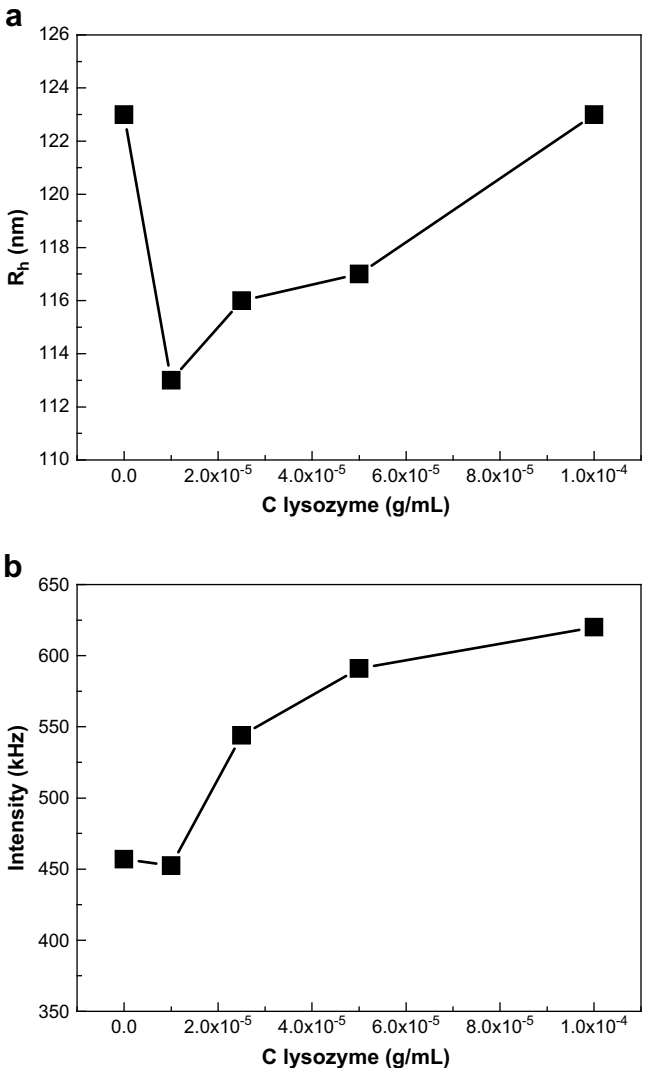

Fig. 10. Hydrodynamic radius distribution (a) and light scattering intensity at 90^0 (b) versus lysozyme concentration for the BS-SCI/Au/lysozyme complexes at 0.01 M salt (concentration of hybrid CSI-BSI/Au was kept constant at 1×10^{-4} g/mL).

The light scattering intensity increased with increasing the lysozyme concentration and reached a plateau close to $c_{\text{lysozyme}} = 1 \times 10^{-4}$ g/mL (Fig. 10b), suggesting an increase in the mass of the nanoensemble, due to complexation of lysozyme [43]. Thus, a complex protein carrier system including an AuNP based marker can be formed.

As observed by UV–vis measurements, upon increasing the concentration of lysozyme, a decrease in the intensity of the AuNPs' surface plasmon resonance band was observed (Fig. 11). The decrease cannot be understood clearly at the moment, but it may be due to some sort of interaction between the Au particles and the protein within the micellar corona. The increase of the scattering due to the presence of lysozyme was expected since the SPR band of the nanoparticles is dependent not only on the size and shape of AuNPs but also on the environment that it surrounds them (and consequently depends on the dielectric constant of the medium [47]).

The dependence of the absorption intensity of the BS-SCI/Au/lysozyme complex nanoensemble on the concentration of lysozyme (see also inset in Fig. 11) paves the way for the utilization of the BS-SCI/Au hybrid colloidal system as a component of a biosensor system. Its functionality could be based on a simple measurement of

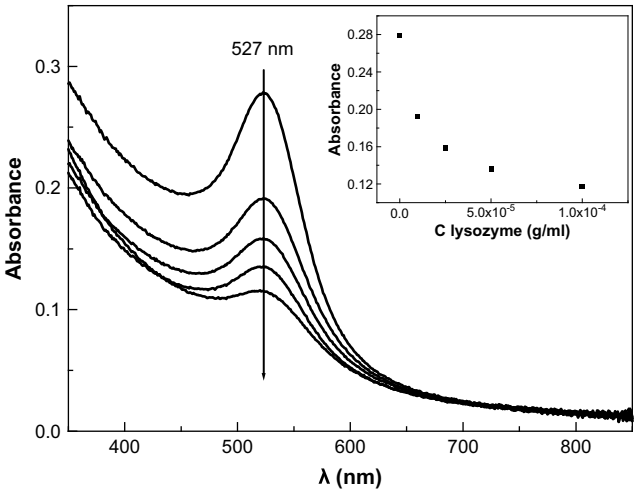

Fig. 11. Absorption spectra for BS-SCI/Au/lysozyme complexes at increasing lysozyme concentration (concentration of BS-SCI/Au hybrid was kept constant at 1×10^{-4} g/mL). Inset, absorption values at peak maximum for BS-SCI/Au/lysozyme complexes versus lysozyme concentration.

the absorption of the complex polymer/AuNPs/protein system, allowing for the determination of the concentration of the protein present in the solution.

4. Conclusions

Au nanoparticles were formed through polymer induced reduction of gold ions within the corona of poly[*tert*-butylstyrene-*b*-sodium (sulfamate-carboxylate-isoprene)] (BS-SCI) micelles in water. Temperature accelerates the formation of Au nanoparticles, however, once the Au reduction is complete no effect on the stability of the BS-SCI/Au colloidal material was noticed. The complex BS-SCI/AuNPs hybrid colloid displayed reversible pH sensitivity, due to the chemical/polyelectrolyte structure of the SCI corona block, taking a more compact conformation under acidic conditions, and a more loose one under alkaline conditions. These structural changes resulted in changes in the optical properties, observed via shifts in the SPR band of the system, due to changes in the AuNP interparticle distances. An increase in the ionic strength of the solution promoted agglomeration of AuNPs within the corona. Finally, lysozyme could be complexed with the BS-SCI/Au colloid resulting in a multifunctional protein carrier system that also includes a metal nanoparticle based marker.

Acknowledgments

The authors acknowledge financial support from the Greek General Secretariat for Research and Technology, Ministry of Development, through the PENED NYVRIPHOS grant (No 03EΔ888). The authors thank Mrs D. Achilleos and Prof. M. Vamvakaki for the TEM measurements, and Dr. E. Karoutsos for the AFM measurements.

References

[1] Eustis S, El-Sayed MA. Chem Soc Rev 2006;35:209–17.
[2] Manea F, Houillon FB, Pasquato L, Scrimin P. Angew Chem Int Ed 2004; 43:6165–9.
[3] Thomas KG, Kamat PV. Acc Chem Res 2003;36:888–98.
[4] Filali M, Meier MAR, Schuber US, Gohy JF. Langmuir 2005;21:7995–8000.
[5] Li J, Shi L, An Y, Li Y, Chen X, Dong H. Polymer 2006;47:8480–7.
[6] Zheng P, Jiang X, Zhang X, Zhang W, Shi L. Langmuir 2006;22:9393–6.
[7] Mosser S, Spatz JP, Moller M, Aberle T, Schmidt J, Burchard W. Macromolecules 2000;33:4791–8.
[8] Meristoudi A, Pispas S, Vainos N. J Polym Sci Part B Polym Phys 2008;46:1515–24.

[9] Teranishi T, Kiyokawa I, Miyake M. Adv Mater 1998;10:596–9.
[10] Leff DV, Brandt L, Heath JR. Langmuir 1996;12:4723–30.
[11] Iwamoto M, Kuroda K, Zaporojtchenko V, Hayashi S, Faupel F. Eur Phys J D 2003;24:365–7.
[12] Alexandridis P, Sakai T. Mater Lett 2006;60:1983–6.
[13] Shukla R, Bansal V, Chaudhary M, Basu A, Bhonde RR, Sastry M. Langmuir 2005;21:10644–54.
[14] Huang X, Jain PK, El-Sayed IH, El-Sayed MA. Nanomedicine 2007;2:681–93.
[15] Newman JDS, Blanchard GJ. Langmuir 2006;22:5882–7.
[16] Mill G, Longenbeger L. J Phys Chem 1995;99:475–8.
[17] Aslam M, Fu L, Vijayamohanan K, Dravid VP. J Mater Chem 2004;14:1795–6.
[18] Kim K, Bong Lee H, Won Lee J, Kun Park H, Soo Shin K. Langmuir 2008;24:7178–83.
[19] Antonietti M, Forster S. Adv Mater 1998;10:195–217.
[20] Alexandridis P, Sakai T. Chem Mater 2006;18:2577–83.
[21] Alexandridis P, Sakai T. Nanotechnology 2005;16:S344–53.
[22] Antonietti M, Wenz E, Bronstein LM, Seregina MS. Adv Mater 1995;7:1000–5.
[23] Sperling RA, Rivera Gill P, Zhang F, Zanella M, Parak WJ. Chem Soc Rev 2008;37:1896–908.
[24] Chen X, Liu Y, An Y, Lü J, Li J, Xiong D, et al. Macromol Rapid Commun 2007;28:1350–5.
[25] Chen X, An Y, Zhao D, He Z, Cheng J, Shi L. Langmuir 2008;15:8198–204.
[26] Xu H, Xu J, Jiang X, Zhu Z, Rao J, Yin J, et al. Chem Mater 2007;19:2489–94.
[27] Zhao H, Douglas EP. Chem Mater 2002;14:1418–23.
[28] Hou G, Zhu L, Chen D, Jiang M. Macromolecules 2007;40:2134–40.
[29] Lu Y, Mei Y, Schrinner M, Ballauff M, Moller MW, Breu J. J Phys Chem C 2007;111:7676–81.
[30] Gupta S, Uhlmann P, Agrawal M, Chapuis S, Oertel U, Stamm M. Macromolecules 2008;41:2874–9.
[31] Gupta S, Uhlmann P, Agrawal M, Lesnyak V, Gaponik N, Simon F, et al. J Mater Chem 2008;18:214–20.
[32] Kawaguchi H. Prog Polym Sci 2000;25:1171–210.
[33] Wittemann A, Haupt B, Merkle R, Ballauf M. Macromol Symp 2003;191:81–8.
[34] Mirkin CA, Letsinger RL, Mucic RC, Storhoff JJ. Nature 1996;382:607–9.
[35] Elghanian R, Storhoff JJ, Mucic RC, Letsinger RL, Mirkin CA. Science 1997;277:1078–81.
[36] Klar TA. In: Shalaev V, Kawata S, editors. Nanoparticles with surface plasmons. The Netherlands: Elsevier; 2007. p. 219–70.
[37] Raschke G, Kowarik S, Franzl T, Sonnichsen C, Klar TA, Feldmann J, et al. Nano Lett 2003;3:935–8.
[38] Hadjichrisitidis N, Iatrou H, Pispas S, Pitsikalis M. J Polym Sci Part A Polym Chem 2000;38:3211–34.
[39] Uhrig D, Mays JW. J Polym Sci Part A Polym Chem 2005;43:6179–222.
[40] Pispas S. J Polym Sci Part A Polym Chem 2006;44:606–13.
[41] Sun X, Jiang X, Dong S, Wang E. Macromol Rapid Commun 2003;24:1024–8.
[42] Li D, He Q, Yang Y, Möhwald H, Li J. Macromolecules 2008;19:7254–6.
[43] Pispas S. J Polym Sci Part A Polym Chem 2007;45:509–20.
[44] Radeva T. Physical chemistry of polyelectrolytes. New York: Marcel & Dekker Inc.; 2001.
[45] Miyamoto D, Oishi M, Kojima K, Yoshimoto K, Nagasaki Y. Langmuir 2008;9:5010–7.
[46] Oishi M, Hayashi H, Uno T, Ishi T, Iijima M, Nagasaki Y. Macromol Chem Phys 2007;208:1176–82.
[47] Nuopponen M, Tenhu H. Langmuir 2007;23:5352–7.